SUPPLEMENTARY INFORMATION FOR:

Direct Measurement of the Surface Energy of Graphene

Christian D. van Engers[1,2], Nico E.A. Cousens[1], Vitaliy Babenko[2,3], Jude Britton[2], Bruno Zappone[4], Nicole Grobert[2] and Susan Perkin[1]*

1) Department of Chemistry, University of Oxford, South Parks Road, Oxford OX1 3QZ, United Kingdom

2) Department of Materials, University of Oxford, Parks Road, Oxford OX1 3PH, United Kingdom

3) Centre for Advanced Photonics and Electronics, Cambridge University, 9 JJ Thomson Ave, Cambridge, CB3 0FA, United Kingdom.

4) Consiglio Nazionale delle Ricerche, Istituto di Nanotecnologia (CNR-Nanotec), c/o Department of Physics, Università della Calabria, Rende (CS) 87036, Italy

*E-mail: susan.perkin@chem.ox.ac.uk

KEYWORDS: Surface Force Balance, Surface Force Apparatus, Graphene, Surface Energy, Adhesion Energy, Energy of Cohesion

Table of Contents

1. Graphene growth and transfer 3

2. Optical Profilometry 13

3. Relation between secondary fringe curvature R_S and surface curvature R_G 14

4. Calculation of contact diameter based on JKR-theory 17

5. Contact angle measurements 18

6. References 19

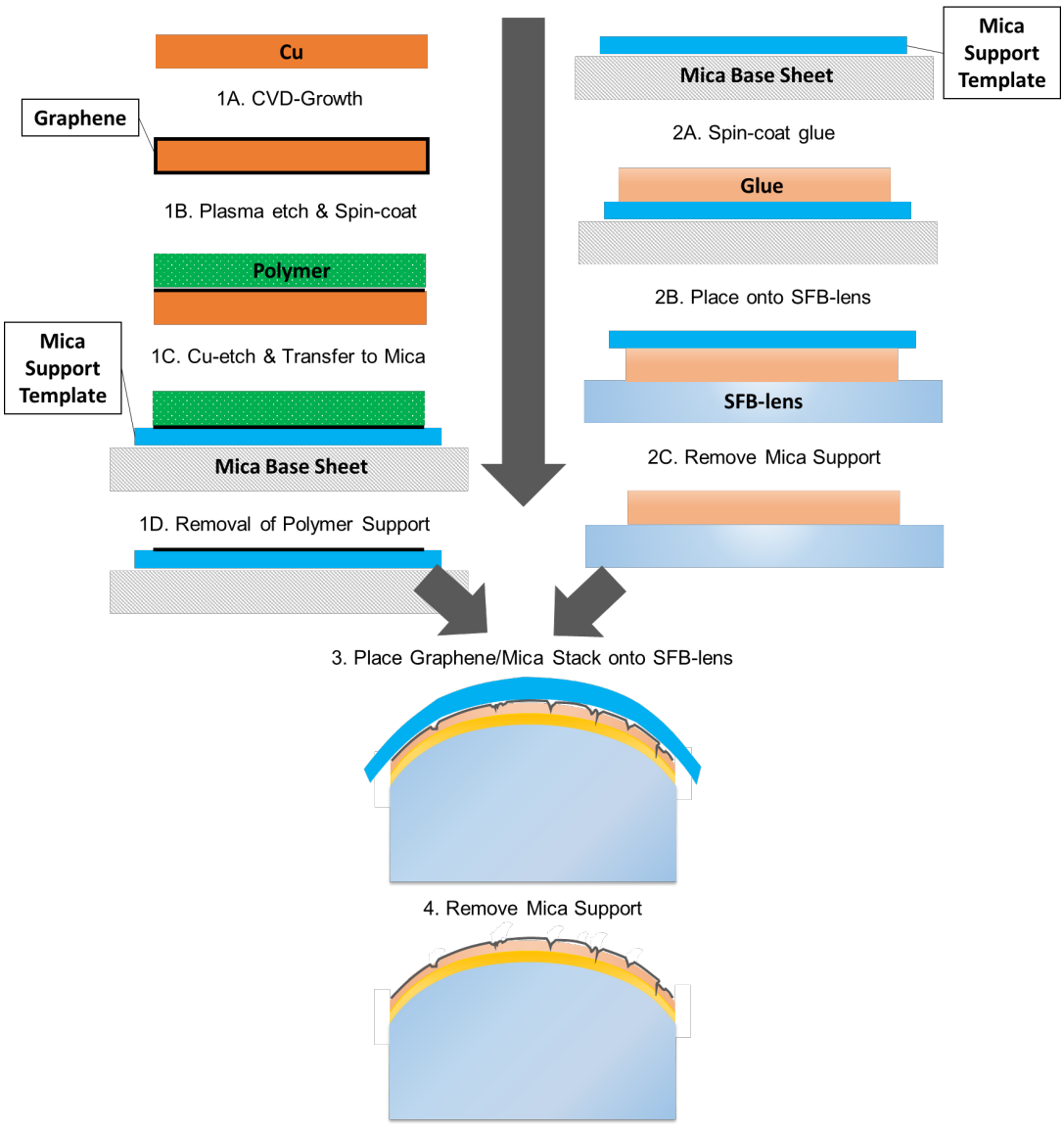
1. Graphene growth and transfer

Summary

A summary of the graphene growth and transfer procedure is given in figure S1. The text will refer to figure S1 as e.g. S1-1A for step 1A: growth of CVD-graphene. Typically, we require an area of ~ 1.5 cm^2 graphene to prepare a single graphene coated SFB-lens. Note that the transfer has been altered since the first publication of the method in 2014[18].

After the graphene growth and transfer procedure, the measurements are performed with a surface force balance (SFB)[19].

Note: Great care was taken to reduce the chance of particulates and contaminants entering the system. After graphene growth all procedures apart from analysis were performed either in a cleanroom (ISO 7, class 10000) or laminar flowhood (ISO14644-1, ISO 5, class 100) environment. Unless noted otherwise, glassware was cleaned in Piranha solution (H2O2 : H2SO4 = 1:3)(Fischer Chemical, >30% w/v, laboratory reagent grade; Fischer Chemical > 95%, analytical reagent grade) prior to use, tools were first degreased with 2-propanol (Sigma Aldrich, puriss., ≥ 99.5%) and chloroform (Sigma Aldrich, Reagentplus, ≥ 99.8%), passivated with 4 M HNO_3 and rinsed with ultrapure water from a Sartorius® water purification system (18.2 MΩ, ≤ 3.5 ppb TOC).



Supplementary Figure S1. Cartoon detailing different steps involved in the fabrication process to eventually yield graphene covered SFB-lenses.

CVD Growth of Single Layer Graphene (SLG) (S1-1A)

Cu foil (99.8%, 25 μm, Alfa Aesar) was first degreased with acetone (Sigma Aldrich, puriss. ≥ 99.5%) and subsequently cleaned by electropolishing in a degassed mixture of 100 mL deionized water, 50 mL ortho-phosphoric acid (Sigma Aldrich, ACS reagent, ≥85 wt. % in H2O), 50 mL ethanol (Fischer Scientific UK, analytic reagent grade), 10 mL 2-propanol, 1 g urea (Sigma Aldrich, ACS reagent, 99.0-100.5%) at 4.5 V for 1 minute[20]. The foil was then placed onto an Al_2O_3 plate inside a quartz tube (100 mm diameter) in a single stage tube furnace. After flushing the tube with Ar, the foil was moved into the hotzone (1060 °C) through the movement of the entire furnace by a motorized stage. The foil was annealed in a mixture of 2.5% H_2/Ar, with a flowrate of 500 sccm for 2 hours. For the synthesis stage, a 250 ppm CH_4/Ar flow was added at 20 sccm initially, and increased by 2 sccm every 20 mins, for 3 hours total synthesis time. The amount of Me/Ar was increased in steps of 0.7 sccm each 30 min. Immediately after, the synthesis was quenched by removing the foil from the hotzone. Finally, the foil was removed after cooling in the H_2/Ar and flushing of the tube with Ar.

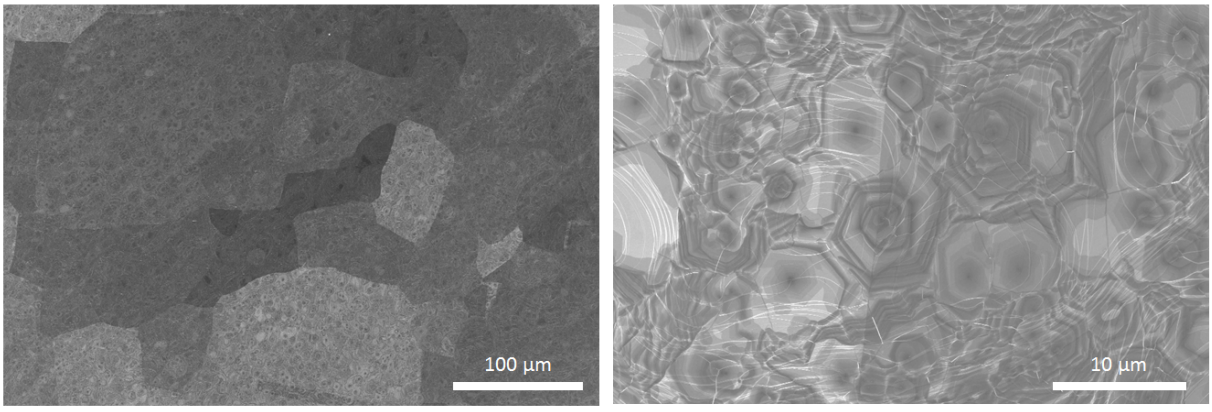
CVD Growth of Few Layer Graphene (FLG) (S1-1A)

Cu foil (99.8%, 25 um, Alfa Aesar) was first degreased with acetone (Sigma Aldrich, puriss. ≥ 99.5%), then sonicated in acetic acid (Sigma Aldrich, puriss., ≥ 99.8%) (45 kHz, 5 min) and placed inside a quartz tube (25 mm diameter) sitting in a single stage tube furnace. After flushing with Ar, the foil was moved into the hotzone (1060 °C) and annealed in H_2 at a flowrate of 500 sccm for 30 min. Graphene was grown by changing to lowering the flowrate of H_2 to 300

sccm and adding methane at a flowrate of 4.15 sccm. After 45 min the reaction was quenched by moving the foil out of the hotzone. After cooling in the synthesis gas and flushing the tube with Ar, the foil was removed.

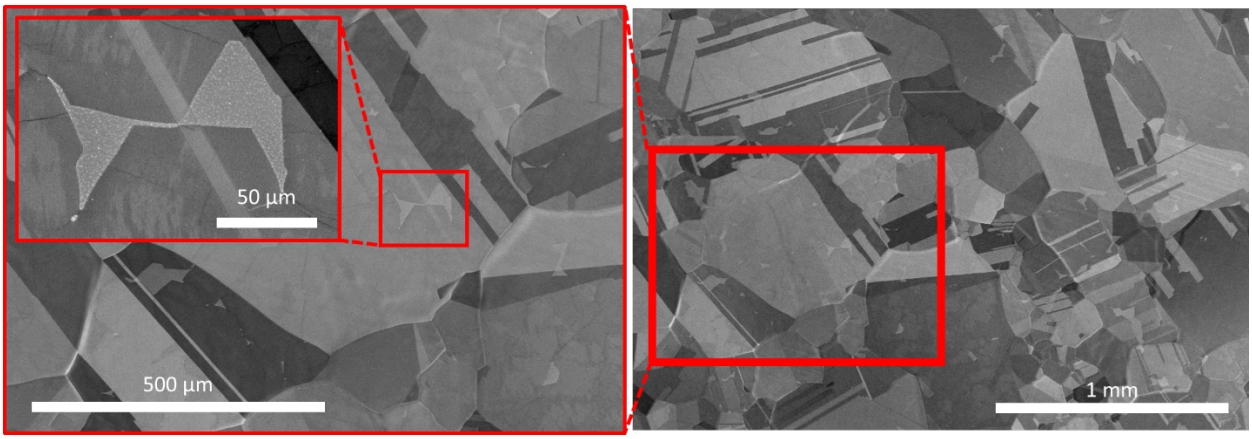
Characterization of Graphene (S1-1A)

Graphene-covered foils were analyzed using SEM (see figure S2-4) (JEOL JSM-6500F, operated at 5 kV), optical microscopy and Raman spectroscopy (figure S5) (JY Horiba LabRAM Aramis Raman spectrometer equipped with a 532 nm laser). Optical microscopy was used to study the coverage. The areas where copper oxidizes show a different color due to interference between the oxidized and underlying layer. By heating the foils to 200˚C for 2 minutes, graphene coverage can be verified to be > 99% (figure S6). Figure S4 shows an SEM image where the growth stopped before the grains had grown together to form a film, giving an estimate of the grain size.

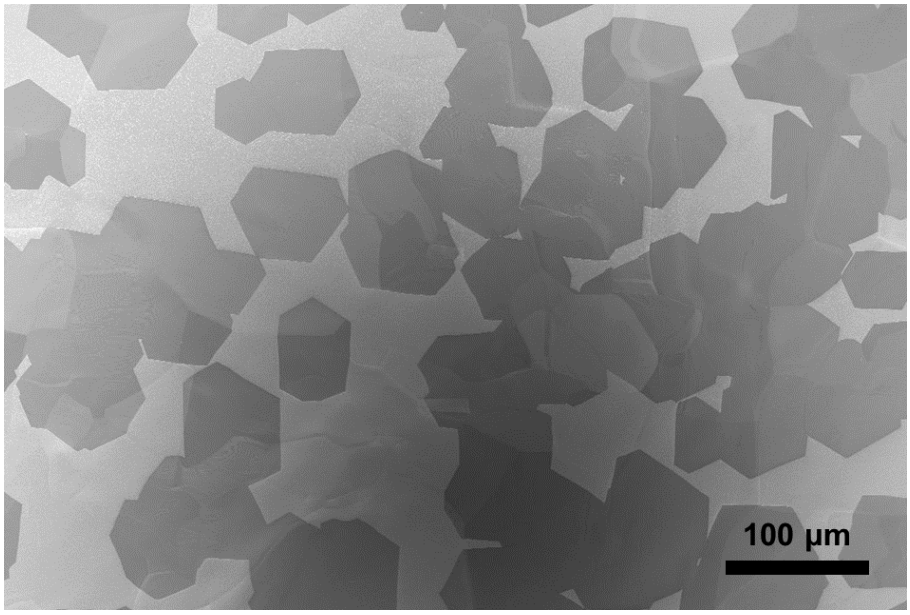


Supplementary Figure S2. SEM micrograph of FLG on copper. The image clearly shows the multilayer structure of FLG (due to the inverted pie growth), different Cu grains, and Cu steps

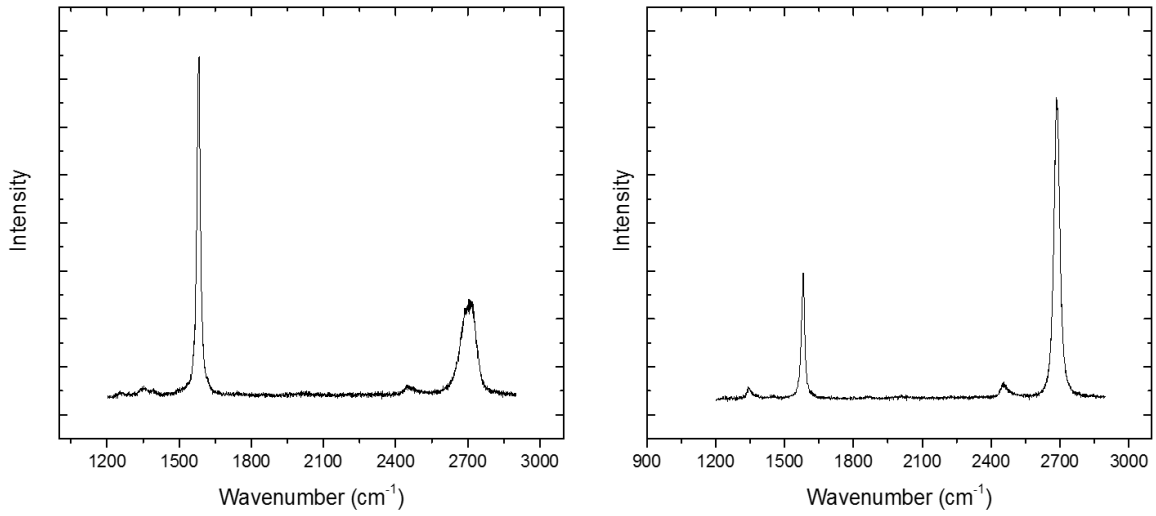
that form due to the high H_2 partial pressure during synthesis. Note that the grain size can be estimated to be 5-10 μm.



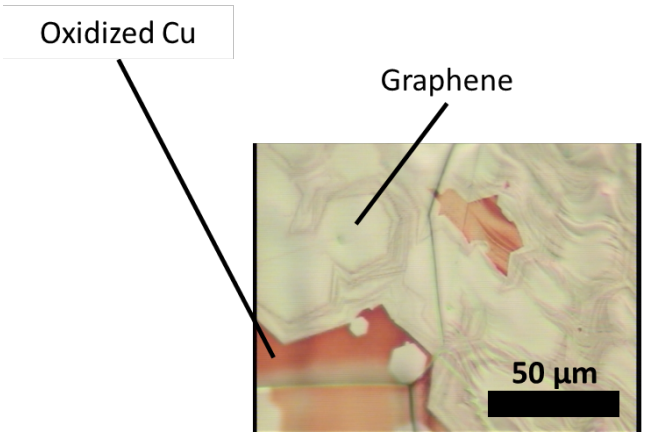
Supplementary Figure S3. SEM micrograph of SLG on Cu. The image clearly shows the Cu grains. The presence of graphene becomes clear due to the contrast variation around non-covered areas.



Supplementary Figure S4. SEM image of single layer graphene islands, grown using the conditions for growing single layer graphene. The growth was stopped prior to the formation of a full film. Note that the grain size can be estimated to be ~ 50 – 100 μm.



Supplementary Figure S5. Raman analysis of FLG (left) and SLG (right) on SiO_2. The 2D-to-G ratio is indicative of multilayer and single layer graphene respectively. The low intensity of the D-peak indicates the graphene grown is of high quality. The low D-peak intensity for the FLG arises due to the (small) size of the laser spot centered at the graphene stack.



Supplementary Figure S6. Image taken using a confocal microscope of a FLG covered copper substrate after heat-treatment. The orange area represents an area not covered by graphene, the beige area represents a graphene-covered area. Also visible are individual graphene hexagons and the underlying copper grain structure.

Graphene Transfer (S1-1B,C,D)

Graphene was transferred according to published procedures[18,22], with some modifications (see figure S1). First, the graphene was removed from one side of the Cu foil by reactive ion etching in O_2 plasma (Oxford Instruments Plasmalab 80, 25 W, 1 min) (S1-1B). Next, pieces of ~ 12 x 12 mm^2 were cut and covered with polystyrene (PS) (Sigma Aldrich, average Mwt. ~ 280,000 by GPC) (0.8 g/mL) by spin-coating at 4000 rpm for 30 s from toluene (Sigma Aldrich, Chromasolv for HPLC, 99.9%) (S1-1B).

The Cu was etched by floating the foils on 0.1 M APS (Sigma Aldrich, reagent grade, 98%). After the copper had been etched away, the graphene/PS stack was picked up using a piranha cleaned piece of PTFE-foil, rinsed in ultrapure water and placed on a piece of freshly cleaved mica (S&J Trading, Inc., ruby mica V-2/V-1 mixed ASTM Grade 1 Optical Grade) (within ~ 2 min) (thickness 3-6 μm) supported by a larger piece of mica (cleaved within 1 h) (S1-1C). When freshly cleaved, mica contains no molecular contaminants, is completely free of particulates and is atomically smooth over the size of a single facet (up to 10 cm^2 in size for ~ 3 μm thick mica)[23].

The mica-base sheet/mica/graphene/PS stack was dried for ≥ 4 h and placed in toluene. The toluene was replaced after 1 h and the sample left overnight in fresh toluene. Finally, the toluene was replaced one final time, the mica-base sheet/mica/graphene stack was rinsed in toluene and left to dry (S1-1D).

We note that for graphene surfaces prepared using polydimethylsiloxane (PDMS) as secondary polymer support during graphene transfer[22], we found the measured surface energy to be drastically lowered to 29 +/- 10 mJ/m^2. Even after rinsing the PDMS stamps with 2-propanol prior to their use as secondary polymer support, we found a value of 48 +/- 10 mJ/m^2. These

results seem to suggest that at least one of the components of the PDMS leeches into solution during graphene transfer and adsorbs to the graphene surface and the use of single component, non-water soluble polymer supports is preferred.

SFB Lens Preparation (S1-2A,B,C)

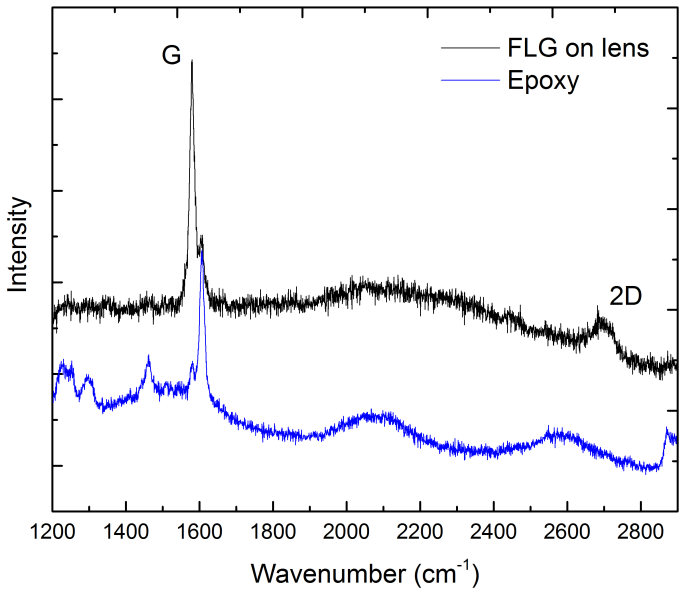
40 nm of Au was evaporated onto 10 mm diameter, 10 mm radius of curvature cylindrical quartz lenses (SFB lenses). After evaporation of the metal layer the lenses were cleaned in a 30 min. aged piranha solution, rinsed with ultrapure water and stored under ethanol. In order to adhere the graphene onto the lenses, the lenses were coated with a uniform layer of epoxy. The coating was prepared by spin-coating Shell EPON resin 1004F (miller-stephenson) from acetone (Arcos Organics, 99.9% for residue analysis) (0.25 g/mL) at 4000 rpm for 30 s onto a 3-6 μm freshly cleaved single mica facet (~ 15 mm x 15 mm) supported by a mica base sheet (S1-2A). After spin-coating the epoxy/mica stacks were annealed for 30 min at 150 °C to reduce residual solvent fraction. Subsequently the epoxy/mica stack was picked up from the heated base-sheet and carefully placed onto the gold-coated SFB lens surface (S1-2B). After cooling the sample down, the mica was peeled off in water revealing a smooth glue surface. Next, the epoxy-coated SFB lens was dried and heated to 150 °C for 30 min to reduce solvent fraction (S1-2C).

Placing the graphene on the SFB lens

The graphene/mica was picked up from the base-sheet it was resting on, and glued graphene face down onto the epoxy-coated lens. Note that the side previously covered in PS is now facing the epoxy (S1-3). Finally, the mica was carefully peeled off in ultrapure water to reveal a clean graphene surface (S1-4). The presence of FLG on the lens, could be verified using Raman

spectroscopy (figure S7). This was not possible in the case of SLG, due to the strong, overlapping Raman signal of the underlying epoxy.

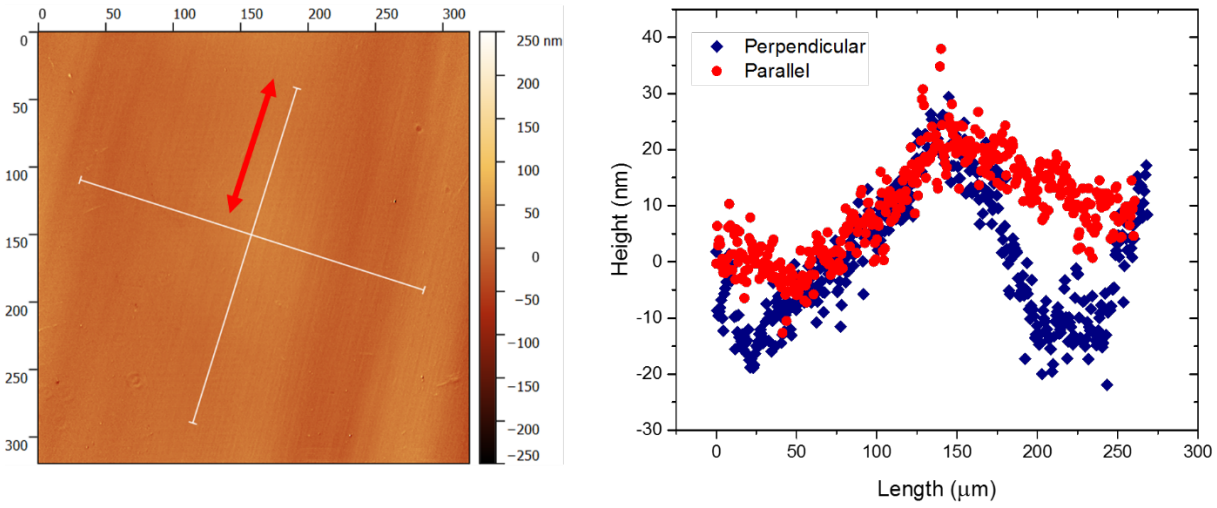
The presence of graphene (and not mica) on the lens could also be qualitatively determined during the fabrication process: Due to the optical transparency and micrometric thickness of the mica support, a single sheet of mica shows a single interference color. Such a mica substrate supporting graphene will thus show a single color, with a dark rectangular area (corresponding to the original shape of the copper growth substrate prior to transfer) indicating the presence of graphene. After removing of the mica from the SFB lens in the final fabrication step, the single mica sheet shows the same color, but a brighter circular area appears in the region from which graphene has been peeled off.



Supplementary Figure S7. Raman spectrum of both FLG covered SFB lens (black), and a SFB lens only covered with epoxy (blue).

2. Optical Profilometry

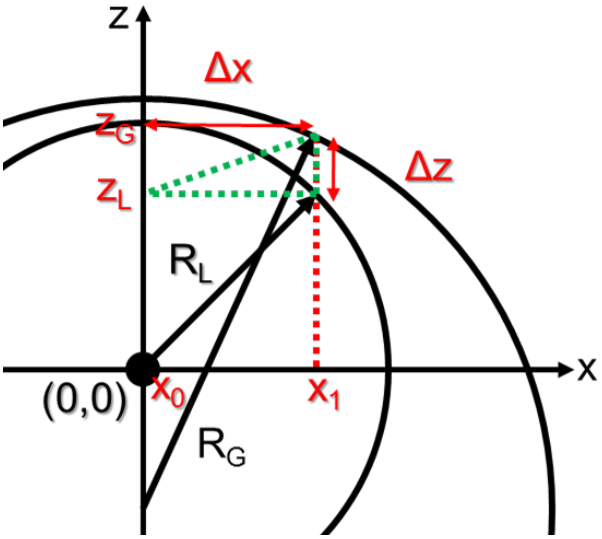
Surface profiling was performed using a Nanofocus μSurf explorer confocal optical profiler with a 50x objective.



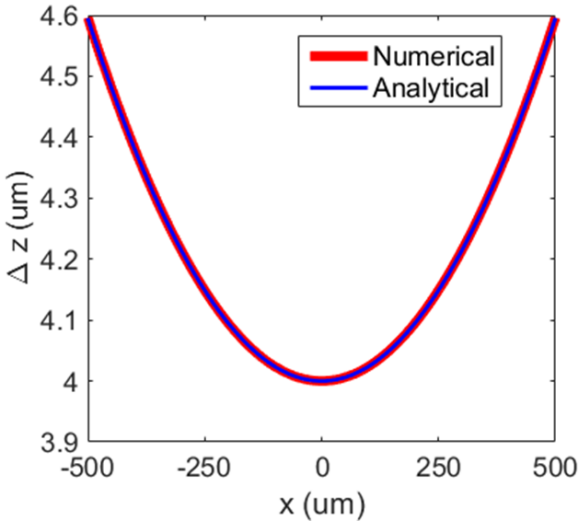
Supplementary Figure S8. Optical profilometry of graphene covered lens surface. The left image shows a background-subtracted optical profilometry image of the graphene covered SFB lens surface. The length scale on the x- and y-axis is in µm. The lens axis is indicated by the double arrow (red). The white lines are drawn parallel and perpendicular to the axis of the cylindrical lens. The corresponding height profiles are given on the right.

3. Relation between secondary fringe curvature $R_{S\square}$ and surface curvature R_G

The relationship between the measured curvature of the lens (R_L) and actual curvature of the graphene surface (R_G) was investigated using a simple numerical calculation based on the cartoon in figure S5. This assumed co-axial alignment, which can be verified directly by inspecting the position of the secondary fringes ($R_{S\square}$) with respect to the primary ones (R_L) and was a prerequisite to be met prior to performing a measurement. We note that in the experiment the correction needed to obtain R_G from R_L is very small, generally in the range $0.9 < R_L/R_G < 1.1$.



Supplementary Figure S9. Schematic showing a side-on view the surface geometry of a cylindrical lens with radius R_L with an overlaying layer of glue. The resulting surface curvature is R_G.



Supplementary Figure S10. Calculated height difference Δz as a function of displacement x. The numerical result is shown in red. The result using the second order Taylor expansion is given in blue.

The analytical expression relating $R_{S\square}$(for convenience from here on referred to as R_S), R_G and R_L is derived by approximating the cylindrical lens as a sphere of radius R_L and the graphene

surface as an overlying sphere with radius R_G. The secondary fringes with curvature R_S result from the height difference between the two. The height difference Δz as a function of displacement along the x direction for a lens with R_L = 10 mm, R_G = 10.5 mm, is shown in figure S10 (numerical). We also derive an analytical expression to relate the three radii (see below for derivation): $R_S = \left(\frac{1}{R_L} - \frac{1}{R_G}\right)^{-1} = -\frac{R_G R_L}{R_G - R_L}$. To arrive at this result we use a second order Taylor expansion. The validity of this approximation is verified in figure S10 (analytical).

Using the schematic in figure S9:

$\Delta x = x_1 - x_0$; $x_0 = 0$

$\Delta x = x_1$

$\Delta z = z_G - z_L$; $z_L^2 = R_L^2 - \Delta x^2$

; $z_G^2 = R_G^2 - \Delta x^2$

Using second order Taylor expansion around x = 0 (since we evaluate $\Delta x \ll R_L$):

; $z_L \approx R_L - \frac{\Delta x^2}{2R_L}$

; $z_G \approx R_G - \frac{\Delta x^2}{2R_G}$

$\Delta z = z_G - z_L = \frac{x^2}{2}\left(\frac{1}{R_L} - \frac{1}{R_G}\right) + R_G - R_L$

The radius of curvature of an arc with height H and width W can be described as:

$R_{arc} = \frac{W^2}{8H} + \frac{H}{2}$; $W \gg H,\ W = 2x_1$

$R_{arc} = \frac{{x_1}^2}{2H}$; $H = \Delta z(x_1) - \Delta z(x_0)$

$H = \frac{{x_1}^2}{2}\left(\frac{1}{R_L} - \frac{1}{R_G}\right) + R_G - R_L - \left(\frac{{x_0}^2}{2}\left(\frac{1}{R_L} - \frac{1}{R_G}\right) + R_G - R_L\right)$

$H = \frac{{x_1}^2}{2}\left(\frac{1}{R_L} - \frac{1}{R_G}\right)$

$$R_{arc} = \left(\frac{1}{R_L} - \frac{1}{R_G}\right)^{-1} \quad ; \qquad R_{arc} = R_S$$

$$R_S = \left(\frac{1}{R_L} - \frac{1}{R_G}\right)^{-1} = -\frac{R_G R_L}{R_G - R_L}$$

4. Calculation of contact diameter based on JKR-theory

Recent reports have challenged the validity of JKR theory for the consideration of layered systems, such as the three-layered mica-based SFB[1,2]. However, for our elastic-rigid (epoxy supported graphene on fused silica SFB lens) two-layered system, equation 1 remains valid[3].

According to JKR-theory, the relation between the contact diameter d and the applied load F is:

$$(d/2)^3 = (R/K) * (F + 6\pi R\gamma + \sqrt{12\pi R\gamma F + (6\pi R\gamma)^2})$$

Where R is the radius of curvature of the surfaces, γ is the surface energy and K is the effective modulus given by:

$$K = \frac{4}{3}\left(\frac{1-v_1^2}{E_1} + \frac{1-v_2^2}{E_2}\right)^{-1}$$

Where v is poisson's ratio and E is the elastic modulus. For two EPON-surfaces coming into contact under zero applied load (i.e. the situation in our system, prior to unloading, using v_{EPON} = 0.495, E_{EPON} = 3.4*10^9 N/m^2 as measured by McGuiggan et al.[1], R = 0.01 m, γ = 0.118 mJ/m^2 we find the contact diameter at F = 0 to be:

$$d_{F=0} = 106\ \mu m$$

And for the contact diameter upon separation (using $F = 3\pi R\gamma$):

$$d_{sep} = 67\ \mu m$$

5. Contact angle measurements

Contact angles were measured on planar surfaces. The preparation procedure is similar to what is mentioned for the growth and transfer of graphene lenses, however, instead of a SFB lens, a 25 mm x 25 mm glass slide is used, with a spin-coated layer of glue on top. This avoids the application of the mica templated glue layer (step 2A,B,C in figure S1).

Static contact angle measurements were performed using a First Ten Angstroms 1000 Drop Shape Instrument (goniometer). For the measurement of the static contact angles, the mica was removed from the glass slide substrates in ultrapure water (revealing the graphene surface), dried on a hotplate and placed on the stage of the goniometer. Subsequently, 5 µL of ultrapure water was dispensed and carefully touched down to the surface on 5 different locations of the substrate. The listed contact angles are an average of these 5 measurements, which were all in very close agreement.

The Young-Dupré equation shows qualitative agreement between the measured jump values and contact angles data, using:

$$\gamma_{Graphene-Air} = \gamma_{Graphene-Water} + \gamma_{Water} * \cos(\theta_{Graphene-Water})$$

6. References

(1) McGuiggan, P. M.; Wallace, J. S.; Smith, D. T.; Sridhar, I.; Zheng, Z. W.; Johnson, K. L. *J. Phys. D. Appl. Phys.* **2007**, *40* (19), 5984–5994.

(2) Math, S.; Horn, R.; Jayaram, V.; Biswas, S. K. *J. Coll. Interf. Sci.* **2007**, *308* (2), 551–561.

(3) Onur Sergici, A.; Adams, G. G.; Müftü, S. *J. Mech. Phys. Solids* **2006**, *54* (9), 1843–1861.

(4) Li, P.; You, Z.; Cui, T. *Sensors Actuators, A Phys.* **2014**, *217*, 56–61.

(5) Koren, E.; Rawlings, C.; Knoll, A. W.; Duerig, U. *Science* **2015**, *348* (6235), 679–684.

(6) Wang, W.; Dai, S.; Li, X.; Yang, J.; Srolovitz, D. J.; Zheng, Q. *Nat. Commun.* **2015**, *6*, 7853.

(7) Girifalco, L. A.; Lad, R. A. *J. Chem. Phys.* **1956**, *25*, 693.

(8) Schrader, M. E. *J. Phys. Chem.* **1980**, *84*, 2774.

(9) Benedict, L. X.; Chopra, N. G.; Cohen, M. L.; Zettl, a; Louie, S. G.; Crespi, V. H. *Chem. Phys. Lett.* **1998**, *286* (5-6), 490–496.

(10) Zacharia, R.; Ulbricht, H.; Hertel, T. *Phys. Rev. B - Condens. Matter Mater. Phys.* **2004**, *69* (15), 1–7.

(11) Björkman, T.; Gulans, A.; Krasheninnikov, A. V.; Nieminen, R. M. *Phys. Rev. Lett.* **2012**, *108*, 1–5.

(12) Lebègue, S.; Harl, J.; Gould, T.; Ángyán, J. G.; Kresse, G.; Dobson, J. F. *Phys. Rev. Lett.* **2010**, *105* (19), 196401.

(13) Spanu, L.; Sorella, S.; Galli, G. *Phys. Rev. Lett.* **2009**, *103* (19), 1–4.

(14) Ziambaras, E.; Kleis, J.; Schröder, E.; Hyldgaard, P. *Phys. Rev. B - Condens. Matter Mater. Phys.* **2007**, *76* (15), 1–10.

(15) Hasegawa, M.; Nishidate, K.; Iyetomi, H. *Phys. Rev. B* **2007**, *76* (11), 1–8.

(16) Chakarova-Käck, S. D.; Schröder, E.; Lundqvist, B. I.; Langreth, D. C. *Phys. Rev. Lett.* **2006**, *96*, 1–4.

(17) Kolmogorov, A. N.; Crespi, V. H. *Phys. Rev. B* **2005**, *71* (23), 1–6.

(18) Britton, J.; Cousens, N. E. A.; Coles, S. W.; Engers, C. D. Van; Babenko, V.; Murdock, A. T.; Koo, A.; Perkin, S.; Grobert, N. *Langmuir* **2014**, *30*, 11485–11492.

(19) Kumacheva, E.; Klein, J. *J. Chem. Phys.* **1998**, *108* (16), 7010.

(20) Yan, Z.; Lin, J.; Peng, Z.; Sun, Z.; Zhu, Y.; Li, L.; Xiang, C.; Samuel, E. L.; Kittrell, C.; Tour, J. M. *ACS Nano* **2012**, *6* (10), 9110–9117.

(21) Zhang, X.; Wang, L.; Xin, J. H.; Yakobson, B. I.; Ding, F. *J. Am. Chem. Soc.* **2014**, *136* (8), 3040–3047.

(22) Song, J.; Kam, F.-Y.; Png, R.-Q.; Seah, W.-L.; Zhuo, J.-M.; Lim, G.-K.; Ho, P. K. H.; Chua, L.-L. *Nat. Nanotechnol.* **2013**, *8* (5), 356–362.

(23) Perkin, S.; Chai, L.; Kampf, N.; Raviv, U.; Briscoe, W.; Dunlop, I.; Titmuss, S.; Seo, M.; Kumacheva, E.; Klein, J. *Langmuir* **2006**, *22* (14), 6142–6152.

(24) Xia, J.; Chen, F.; Li, J.; Tao, N. *Nat. Nanotechnol.* **2009**, *4* (8), 505–509.